Supplementary Information for "Evidence for origins of soot emissions from the Chicxulub asteroid impact at the Cretaceous–Paleogene boundary"

Shixiong Hu[1], Clay R. Tabor[1], Charles G. Bardeen[2], Owen B. Toon[3], Wendy S. Wolbach[4]
Joshua Coupe[6], Cheryl S. Harrison[7], Nicole S. Lovenduski[6], Kenneth G. MacLeod[5]
Paul J. Markwick[9], Siddhartha Mitra[10], Julio Sepúlveda[6], Robert Kelleher[6] ,and Rachel Wheatley[8]

[1]Department of Earth Sciences, University of Connecticut, Storrs, Connecticut 06269, USA
[2]Atmospheric Chemistry, Observations, and Modeling Laboratory, National Center for Atmospheric Research, Boulder, Colorado 80301, USA
[3]Department of Atmospheric and Oceanic Sciences and Laboratory for Atmospheric and Space Physics, University of Colorado Boulder, Boulder, Colorado 80303-7814, USA
[4]Department of Chemistry and Biochemistry, College of Science and Health, DePaul University, Chicago, Illinois, USA
[5]Department of Geological Sciences, University of Missouri, Columbia, Missouri, USA
[6]Department of Atmospheric and Oceanic Sciences and Institute of Arctic and Alpine Research, University of Colorado Boulder, Boulder, Colorado, USA
[7]Department of Oceanography and Coastal Sciences and Center for Computation and Technology, Louisiana State University, Baton Rouge, Louisiana, USA
[8]Department of Geological Sciences, East Carolina University, Greenville, North Carolina, USA
[9]Knowing Earth Limited, Otley LS21 3JP, United Kingdom
[10]Virginia Institute of Marine Science, Gloucester Point, VA 23062, USA

Contents

Supplementary Methods; Supplementary Figures 1–4; Supplementary Tables 1–2.

Supplementary Methods

Evaluating modeled carbon deposition

We quantified the discrepancies of each simulation and for the sites from the Wolbach records, which are treated as reference values. For each site, the model-proxy residual is defined as d_i. For each simulation, we calculated the mean squared error (MSE) and the root mean squared error (RMSE). A negative bias (b) indicates underestimation of the model, whereas a positive bias indicates overestimation. Following the decomposition of MSE, we define the irreducible error as e. Calculations used in the model-proxy comparison are:

$$d_i = X_{model,i} - X_{proxy,i}$$

$$MSE = \frac{1}{n}\sum_{i=1}^{n} d_i^2 = \frac{1}{n}\sum_{i=1}^{n} (X_{model,i} - X_{proxy,i})^2$$

$$RMSE = \sqrt{MSE}$$

$$b = \frac{1}{n}\sum_{i=1}^{n} d_i$$

$$e = \sqrt{MSE - b^2}$$

For total carbon deposition, we calculated uncertainty-weighted metrics from the model–proxy differences, $d_i = X_{model,i} - X_{proxy,i}$, in deposition units. The selected asymmetric error width was

$$\sigma_i = \begin{cases} \sigma_i^+, & d_i > 0, \\ \sigma_i^-, & d_i \le 0, \end{cases}$$

where σ_i^+ and σ_i^- are the upper and lower error-bar widths relative to the proxy central value, in mg cm^{-2}. The upper and lower uncertainties in Supplementary Table 1 are reported as signed deviations from the central value. The reported upper and lower uncertainty deviations were converted to absolute widths before weighting. The upper width was selected when the model exceeded the proxy central value, and the lower width otherwise. Thus, a nonzero selected uncertainty width refers to a positive magnitude, irrespective of the sign used to report the deviation in Supplementary Table 1.

Let m denote the number of sites with nonzero selected uncertainty widths among the $n = 7$ comparison sites. The normalized weights were

$$\alpha_i = \begin{cases} \dfrac{m}{n}\dfrac{\sigma_i^{-2}}{\sum_{j:\,\sigma_j \neq 0} \sigma_j^{-2}}, & \sigma_i \neq 0, \\ \dfrac{1}{n}, & \sigma_i = 0, \end{cases} \qquad \sum_{i=1}^{n} \alpha_i = 1.$$

Sites with nonzero selected uncertainty widths were assigned relative inverse-square weights. At El Kef, the lower uncertainty is omitted in Supplementary Table 1 due to the missing lower bound error bar from Wolbach records.Therefore the unavailable lower uncertainty is encoded as zero in the analysis inputs. When this side was selected, El Kef retained its unweighted site weight of 1/7, while the other six sites shared the remaining weight of 6/7. No uncertainty floor was applied.

The weighted metrics were

$$\mathrm{MSE}_w = \sum_{i=1}^{n} \alpha_i d_i^2, \qquad \mathrm{RMSE}_w = \sqrt{\mathrm{MSE}_w},$$

$$b_w = \sum_{i=1}^{n} \alpha_i d_i,$$

$$e_w = \sqrt{\sum_{i=1}^{n} \alpha_i (d_i - b_w)^2} = \sqrt{\mathrm{MSE}_w - b_w^2}.$$

The weights are dimensionless, so weighted RMSE, bias, and centered residual scatter retain units of mg cm^{-2}.

For Supplementary Table 2, residuals for each proxy variable v were normalized by its across-site sample standard deviation, calculated with $n - 1 = 6$ degrees of freedom for the seven proxy values.

$$s_{proxy,v} = \sqrt{\frac{1}{n-1} \sum_{i=1}^{n} \left(X_{proxy,v,i} - \overline{X}_{proxy,v} \right)^2}.$$

The normalized residuals and metrics were

$$d^*_{v,i} = \frac{X_{model,v,i} - X_{proxy,v,i}}{s_{proxy,v}},$$

$$\mathrm{NRMSE}_v = \sqrt{\frac{1}{n} \sum_{i=1}^{n} (d^*_{v,i})^2}, \qquad b^*_v = \frac{1}{n} \sum_{i=1}^{n} d^*_{v,i},$$

$$e^*_v = \sqrt{\mathrm{NRMSE}_v^2 - (b^*_v)^2}, \qquad \mathrm{NMAE}_v = \frac{1}{n} \sum_{i=1}^{n} |d^*_{v,i}|.$$

These metrics are unweighted and dimensionless. The normalization enables the percentage comparison between the proxy variable v: total carbon deposition and soot fraction.

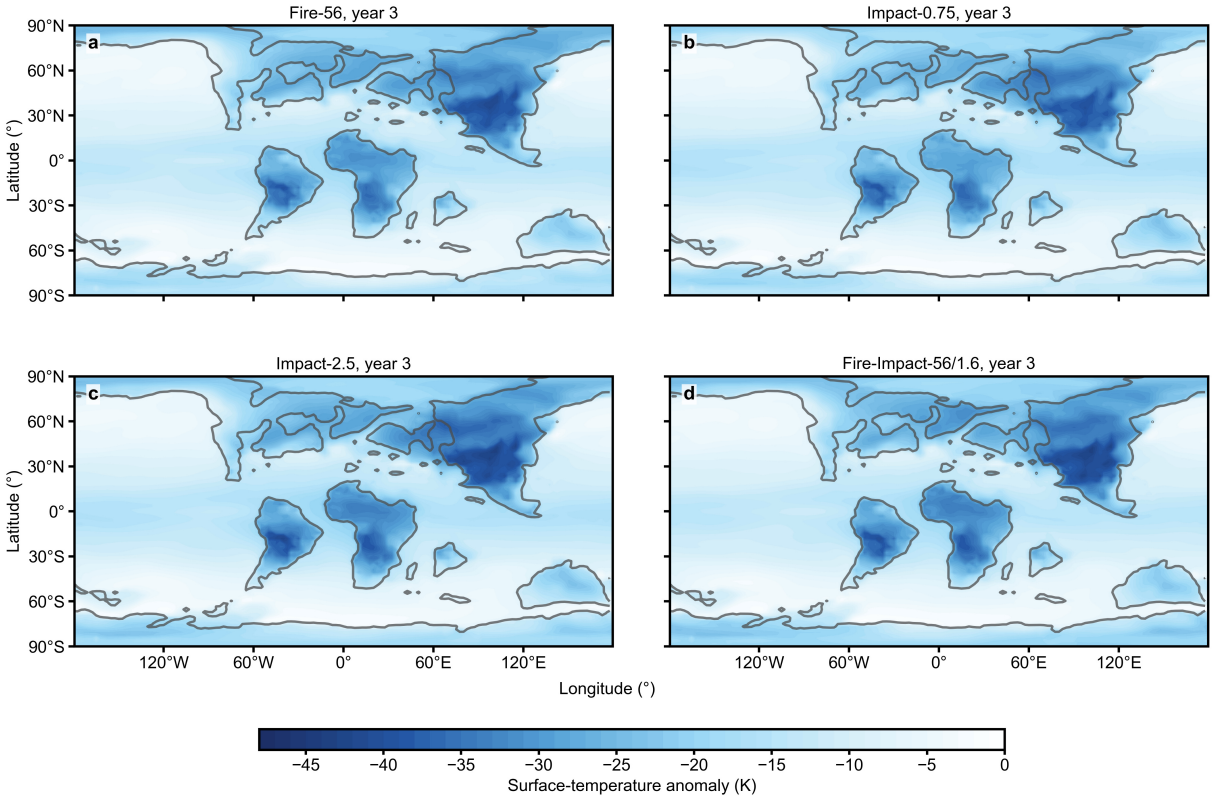
For Table 2, unweighted and weighted total-carbon metrics were expressed as percentages of the same unweighted mean Wolbach deposition across the seven sites,

$$\overline{X}_{proxy,TotC} = \frac{1}{n} \sum_{i=1}^{n} X_{proxy,TotC,i}.$$

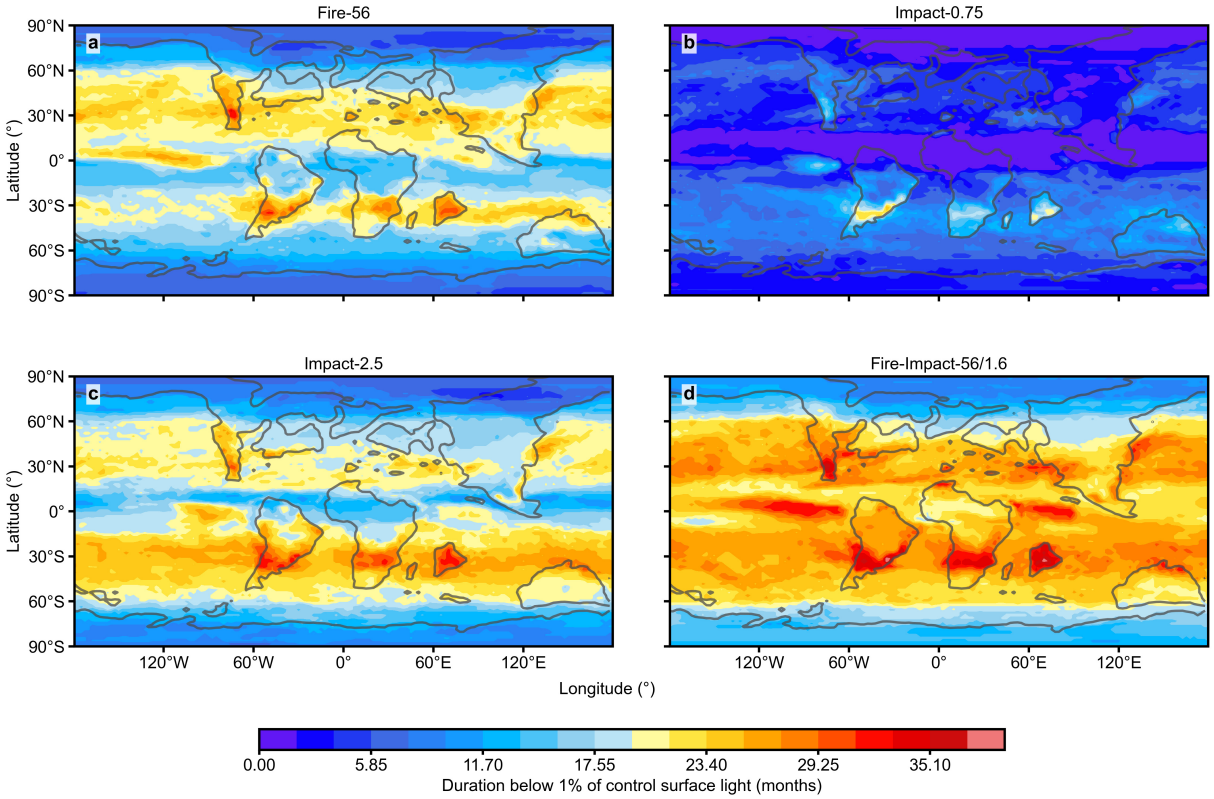
For $Q \in \{\mathrm{RMSE}, b, e\}$,

$$Q_{TotC,\%} = 100 \frac{Q_{TotC}}{\overline{X}_{proxy,TotC}}, \qquad Q_{w,TotC,\%} = 100 \frac{Q_{w,TotC}}{\overline{X}_{proxy,TotC}}.$$

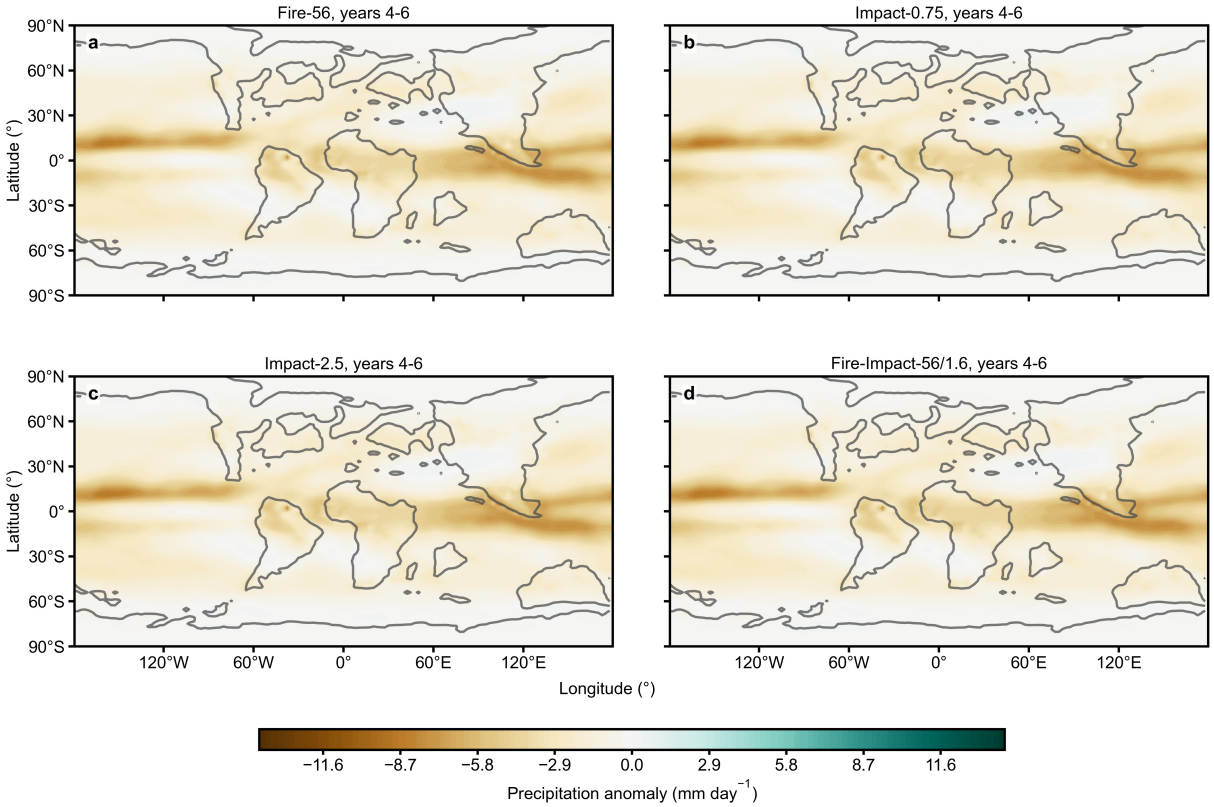
Here, Q_{TotC} and $Q_{w,TotC}$ denote the unweighted and uncertainty-weighted metrics in deposition units, respectively, before normalization by the proxy standard deviation. Unweighted soot-fraction RMSE, bias, and centered residual scatter were similarly divided by the mean proxy soot fraction and multiplied by 100. Calculations used unrounded proxy means. These mean-relative percentages are distinct from the proxy-standard-deviation-normalized metrics in Supplementary Table 2.



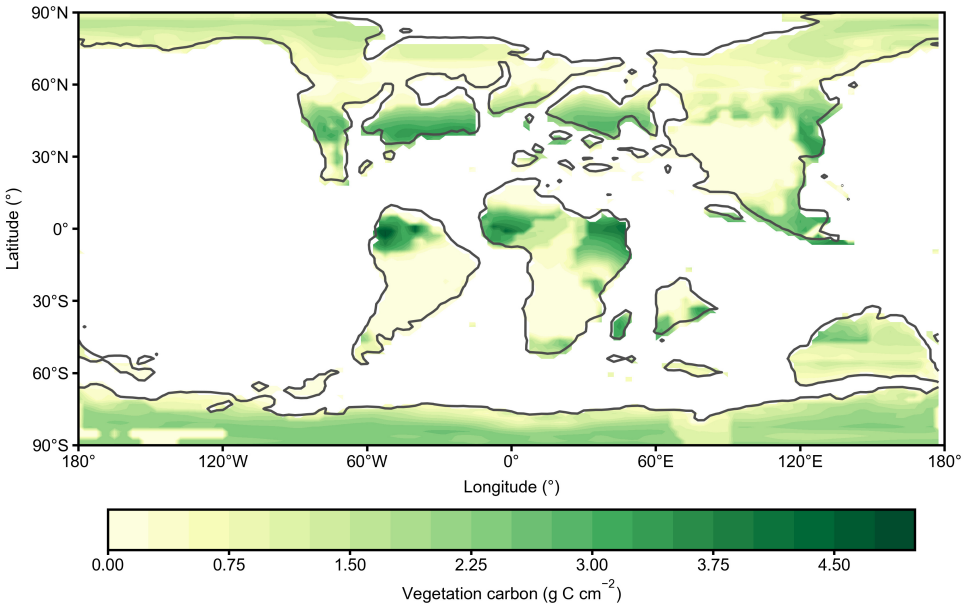
Supplementary Figure 1. Year-3 surface-temperature anomalies. Mean surface-temperature anomaly in simulation year 3 for Fire-56 (a), Impact-0.75 (b), Impact-2.5 (c), and Fire-Impact-56/1.6 (d). Units are K.



Supplementary Figure 2. Duration of strongly reduced surface light. Cumulative months during the first nine post-impact years when downwelling surface shortwave radiation is below 1% of the corresponding control value for Fire-56 (a), Impact-0.75 (b), Impact-2.5 (c), and Fire-Impact-56/1.6 (d).



Supplementary Figure 3. Years 4–6 precipitation anomalies. Mean total-precipitation anomaly over post-impact years 4–6 for Fire-56 (a), Impact-0.75 (b), Impact-2.5 (c), and Fire-Impact-56/1.6 (d). Units are mm day^{-1}.



Supplementary Figure 4. Maastrichtian vegetation carbon. Initial vegetation carbon simulated by the Community Land Model version 4 (CLM4) after conversion from g C m^{-2} to g C cm^{-2}. Units are g C cm^{-2}.

Supplementary Tables

Supplementary Table 1. Processed and raw carbon records at the Cretaceous–Paleogene (K–Pg) boundary.

Site	Total carbon (mg cm^{-2})	Soot fraction (%)
Raw data		
Woodside Creek, NZ	$4.8\ ^{+5}_{-5}$	69
Chancet Rocks, NZ	$35\ ^{+5}_{-20}$	68
Stevns Klint	$11\ ^{+11}_{-1}$	21
Caravaca	$10\ ^{+10}_{-1}$	14
Gubbio	$13\ ^{+13}_{-1}$	17
Agost[1]	$3.6\ ^{+3.8}_{-0}$	2
Raton[1]	$4.0\ ^{+6.5}$	1
El Kef	$15\ ^{+15}$	19
Flaxbourne River, NZ	$1.3\ ^{+0}_{-0.6}$	55
Elendgraben[2]	$0.8\ ^{+8}_{-0}$	12
Sumbar	$13\ ^{+3}_{-3}$	15
DSDP 465[3]	$3.6\ ^{+0.4}_{-0.4}$	50
Processed data		
NZ average	13.7	64
Stevns Klint	11	21
Caravaca	10	14
Gubbio	13	17
El Kef	15	19
Sumbar	13	15
DSDP 465	3.6	50

NZ average is the mean of Woodside Creek, Chancet Rocks, and Flaxbourne River. DSDP denotes Deep Sea Drilling Project. Raw data are from Wolbach et al. (1990), except DSDP Site 465 from Wolbach et al. (2003). Agost, Raton, and Elendgraben were excluded from model comparison. [1]Etched for 600 h to remove resistant kerogen (Agost); Raton contains abundant local coal. [2]H_2O_2 procedure. [3]Wolbach et al. (2003).

Supplementary Table 2. Scale-normalized model–proxy misfit metrics for total carbon deposition and soot fraction.

Variable	Case	Proxy SD	Norm. RMSE	Norm. bias	Norm. MAE
Total carbon deposition	Fire-56	3.791	1.135	-0.508	1.046
Total carbon deposition	Impact-56	3.791	1.348	-0.607	1.277
Total carbon deposition	Fire-Impact-56/2.5	3.791	1.083	-0.513	1.027
Total carbon deposition	Fire-Surface-56	3.791	1.750	-0.939	1.523
Soot fraction	Fire-56	0.200	0.865	-0.270	0.670
Soot fraction	Impact-56	0.200	0.787	-0.258	0.561
Soot fraction	Fire-Impact-56/2.5	0.200	0.841	-0.159	0.671
Soot fraction	Fire-Surface-56	0.200	0.753	0.119	0.671

Residuals were normalized by the across-site standard deviation (SD) of each proxy variable. RMSE denotes root mean squared error; MAE, mean absolute error; and Norm., normalized. The normalized metric columns are dimensionless. Proxy SD is expressed in mg cm^{-2} for total carbon deposition and in fractional units for soot fraction. Negative bias indicates model underprediction relative to the Wolbach record. All metrics are unweighted; the uncertainty weights α_i were not used in this table.

Supplementary References

1. Wolbach, W. S., Gilmour, I. & Anders, E. Major wildfires at the Cretaceous/Tertiary boundary. In *Global Catastrophes in Earth History* 391–400 (Geological Society of America, 1990). `https://doi.org/10.1130/SPE247-p391`.

2. Wolbach, W. S., Widicus, S. & Kyte, F. T. A search for soot from global wildfires in central Pacific Cretaceous–Tertiary boundary and other extinction and impact horizon sediments. *Astrobiology* **3**, 91–97 (2003). `https://doi.org/10.1089/153110703321632444`.